Research on solar radiation error of sounding temperature sensor

Research on solar radiation error of sounding temperature sensor

Hongxia Cao[1,2,3,4,5,*], Minming Liu[5], Xinyu Liu[5], Zengxuan Wang[5], Yan Tang[5]

[1] Key Laboratory of Meteorological Disaster, Ministry of Education, Nanjing, China
[2]Joint International Research Laboratory of Climate and Environment Change, Nanjing, China
[3]Collaborative Innovation Center on Forecast and Evaluation of Meteorological Disaster, Nanjing, China
[4]Jiangsu Key Laboratory of Meteorological observation and Information Processing, Nanjing, China
[5]School of Electronic and Information Engineering, Nanjing University of Information Science and Technology, Nanjing, China

*Corresponding author e-mail: nanshichx@163.com

Abstract. The error of sounding temperature sensor with bead thermistor induced by solar radiation seriously affects the accuracy of temperature measurement. To solve this problem, this paper presents a novel numerical analysis method based on computational fluid dynamics to correct solar radiation error. The error thermal analysis model of sounding temperature sensor with bead thermistor is established from ground to 32km altitude with different air pressures, and computational fluid dynamics is employed for numerical simulation analysis of solar radiation error. The solar radiation errors are reported in different physical parameters such as the altitude, the direction of solar radiation and the surface coating reflectivity of sensor. The results show that the solar radiation errors present a nonlinear monotone increasing trend with the rise of altitude. Among the errors caused by solar radiation, the error is biggest in the direction perpendicular to the front of the sensor. The simulation results also indicate that the solar radiation error can be significantly reduced by improving the surface coating reflectivity of sensor.

1. Introduction

In the field of high altitude meteorological sounding, balloon suspended radiosonde is widely used at home and abroad to detect the vertical profiles of atmospheric temperature, air pressure, humidity and other meteorological elements from the ground to tens of kilometers [1,2]. Bead thermistor is the main sensor for temperature detection on the radiosonde. The error induced by solar radiation is considered to be the main source of temperature measurement error under the condition of sunshine [3,4]. At present, many meteorologists at home and abroad have studied the error of solar radiation. The research methods mainly include wind tunnel experiment method and empirical estimation method, but both of them have shortcomings which can significantly affect the effect of solar radiation error correction [5-7].

Considering the complexity of the specific problem of correcting the solar radiation error of sounding temperature sensor with bead thermistor, a simulated numerical analysis method using computational fluid dynamics (CFD) is proposed in this paper to analyze the solar radiation error. The effects of solar radiation direction and surface coating reflectivity on solar radiation error at different altitudes are systematically studied.

2. Physical Model of Sounding Temperature Sensor

As for the correction of solar radiation error of sounding temperature sensor, the physical model of temperature sensor without support structure has been established before. In this paper, a numerical analysis model of temperature sensor with support structure is established, and the correction of solar radiation error is studied. Fig. 1 is the physical model of a temperature sensor with bead thermistor including a certain support structure. Fig. 1 (a) is the front view of the sensor, and Fig. 1 (b) is a schematic diagram of the bead thermistor. It can be seen from the figure that the frame is a thin rectangular structure with U-shaped openings with its structural parameters are 40mm×20mm×2mm (length×width×thickness). The bead thermistor includes a spherical resistor body, ellipsoidal epoxy insulating layer and leads. The resistor body is wrapped in the insulating layer, and the signal is sent to the radiosonde through the leads for processing.

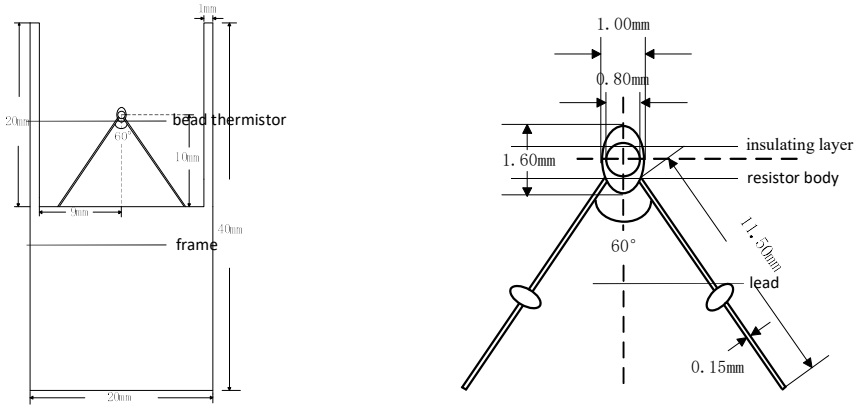

(a) The front view of sensor (b) The schematic diagram of bead thermistor

Figure 1. The physical model of a temperature sensor.

3. Calculation Model of Temperature Sensor and Fluid-solid Coupled Heat Transfer Analysis

3.1. Three-dimension model of temperature sensor

The solar radiation error of sounding temperature sensor is analyzed by using CFD (computational fluid dynamics) method, The whole analytical process including modeling, meshing, steady-state thermal analysis and general post-processing[8-10]. A 3D modeling software Pro/E is used to establish the calculation model of the temperature sensor including bead thermistor and frame shown in Fig. 1, as well as the air domain around the sensor. Considering the external environment of the temperature sensor is an infinite air domain, however, it is impossible to simulate infinite space by building infinite air grids in numerical calculation. For balance calculation efficiency and accuracy, a rectangular air domain of moderate size is established. The size of the air domain is 400mm×200mm×20 mm, which is set as 10 times of the size of the sensor model.

3.2. Mesh generation

Fig. 2 is the grids of the temperature sensor model and the air domain. Fig.2 (a) is the overall grids, the solid part in the middle of the figure is the temperature sensor, and the periphery is the air domain. Fig.2 (b) and (c) are grids of the frame and the bead thermistor, respectively. The temperature sensor has an

irregular shape. Hence the unstructured tetrahedral meshing method with strong adaptability is adopted. Because the local area is treated with meshing densification, the grids of the bead thermistor in Fig. 2 are much smaller than that in the air domain. The calculation model is divided into four regions: inlet, outlet, solid wall and heat exchange module wall.

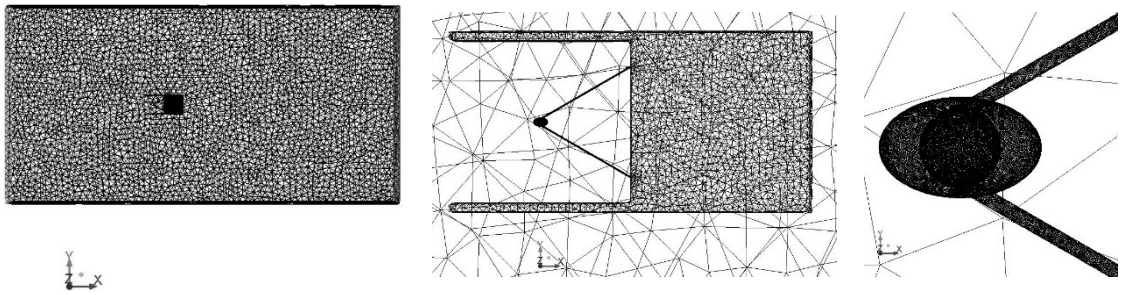

(a) The overall grids (b) The grids of frame (c) The grids of bead thermistor

Figure 2. The grids of temperature sensor model.

3.3. Fluid-solid coupling heat transfer analysis

Boundary conditions are the conditions on the boundary of the fluid motion control equation that should be satisfied. Its setting will have remarkable impact on solution results. The boundary conditions are set as follows. For radiosonde, the relative airflow velocity of the temperature sensor is equal to the rising speed of 6 m/s. Due to low fluid velocity, the ambient air around it can be approximately viewed as incompressible. The pressure-based solver is employed and the air flow is assumed to be steady laminar flow. Energy equation is used for the model that involves radiation, convective heat transfer and thermal conduction. Semi-Implicit Method for Pressure-Linked Equation (SIMPLE) algorithm is utilized for the pressure and speed decoupling. The second-order upwind scheme is adopted to improve the accuracy of calculated results of the momentum, energy and turbulence parameters. The air inlet wall adapts a velocity inlet boundary condition and the air outlet wall features a pressure outlet boundary condition. Because the change of air pressure has a significant impact on the convective heat transfer of the temperature sensor, the relationship between atmospheric pressure and altitude is shown in Fig.3 according to the standard atmosphere of the United States in 1976[11]. As can be seen from Fig. 3, atmospheric pressure decreases gradually with the rise of altitude. Atmospheric pressure was converted into air density, which was set in numerical calculation to represent different altitudes.

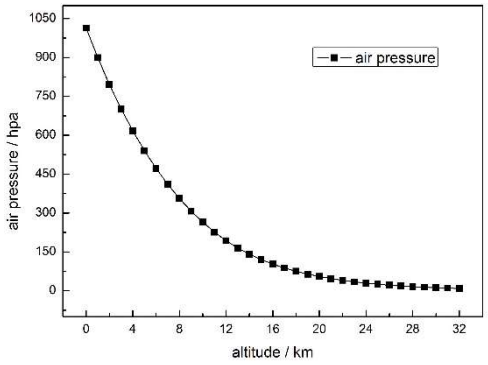

Figure 3. Relationship between atmospheric pressure and altitude

The resistor body and leads of the bead thermistor are set as aluminum trioxide and platinum, respectively. The insulating layer and support frame are set as epoxy. Table 1 shows the physical parameters of the fluid and materials of temperature sensor.

Table 1. The physical parameters of fluid and materials of temperature sensor.

Material	Density / $kg \cdot m^{-3}$	Specific heat / $J \cdot kg^{-1} \cdot K^{-1}$	Thermal conductivity / $W \cdot m^{-1} \cdot K^{-1}$
Air	1.225	1006.43	0.0242
Aluminum trioxide	3900	840	35
Epoxy	980	1200	0.2
Platinum	21450	138	73

4. Results and discussion

4.1. Effect of solar radiation direction on solar radiation error

As is known to all, different flying time and different hanging orientation of the radiosonde will cause corresponding changes in the direction of solar radiation. In order to study the influence of solar radiation direction on temperature measurement, we select three coordinate axes (i.e. X, Y and Z axes) to simulate three different solar radiation directions. The structure and size of the temperature sensor are shown in Fig. 1. The reflectivity of the surface coating is 70%. Fig. 4 (a), (b) and (c) show the temperature field distribution when the sun radiation direction is along X axis(top of sensor), Y axis(side of sensor) and Z axis(front of sensor) direction at altitude of 32km, respectively. The initial value of temperature in numerical calculation is set as atmospheric temperature at 32 km. It can be seen from Fig. 4 that the direction of solar radiation has a significant influence on the temperature field distribution of the sensor. For the part facing the direction of solar radiation receives more radiation, and the heat transfer is slow due to the low thermal conductivity of the material, so the bright region with high temperature appears. By calculating the body average temperature of resistor body, the temperature measurement errors caused by solar radiation are 1.527K, 0.460K and 3.921K, respectively. That is to say, when the sun irradiates along Z direction, the error is the largest, and the measurement error is the smallest along Y direction.

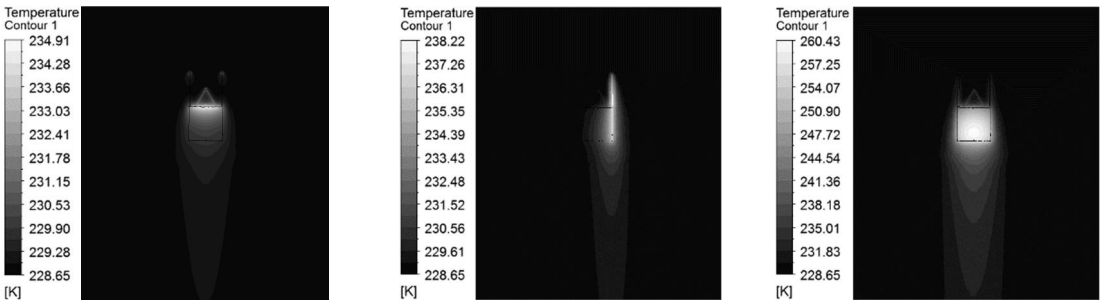

(a)X axis direction (b)Y axis direction (c)Z axis direction

Figure 4. Distribution of the temperature field in different directions of solar radiation

4.2. Effect of reflectivity of surface coating on solar radiation error

In this paper, the influence of coating reflectivity of sensor surface on solar radiation error is studied and compared. The range of reflectivity is from 60% to 90% in our models, where the step length of the reflectivity change is 10%. The structure and size of the sensor are shown in Fig. 1. The temperature field of the sensor is simulated numerically by using CFD while the solar radiation is along X direction. Fig. 5 shows the relationship between altitude and solar radiation error of different surface coating reflectivity from sea level to 32 km altitude. As it can be seen from the figure, the error of solar radiation increases with the rise of altitude. In addition, the higher the reflectivity, the less solar radiation absorbed by the sensor, so the solar radiation error decreases gradually with the increase of the reflectivity.

The solar radiation error numerically calculated are compared with experimental results reported in literature, and comparison shows that the results in this paper are in good agreement with the measured data of WMO[12]. This indicates the validity of the numerical analysis method for solar radiation error correction proposed in this paper.

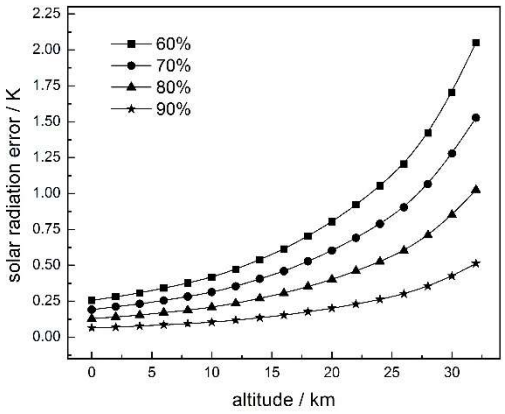

Figure 5. Relationship between altitude and solar radiation errors of different surface coating reflectivity

5. Conclusion

In this paper, the temperature measurement errors caused by solar radiation heating of sounding temperature sensor at altitudes from sea level to 32 km are numerically simulated and analyzed by using CFD method. The effects of solar radiation direction and reflectivity of surface coating on solar radiation error are discussed. The following conclusions are drawn: Solar radiation has a significant influence on temperature measurement of sounding temperature sensor. Therefore, it must be corrected. The error of solar radiation increases with the rise of altitude. The direction of solar radiation has a significant effect on solar radiation error. The solar radiation error decreases with the increase of reflectivity of the surface coating. The numerical results are in good agreement with the experimental data reported in literature.

Acknowledgments

This work was supported by a Project Funded by the Priority Academic Program Development of Jiangsu Higher Education Institutions. Jiangsu student's innovation and entrepreneurship training program. A Project Funded by Jiangsu Key Laboratory of Meteorological observation and Information Processing under Grant No. 2201081301063. A Postdoctoral Project Funded by Jiangsu Province under Grant No. 2191081605001.

References

[1] James K. Luers, Robert E. Eskridge. Use of Radiosonde Temperature Data in ClimateStudies[J]. Journal of climate,1998,11:1002-1019.
[2] Sánchez J. L., Posada R., García-Ortega E., et al. A method to improve the accuracy of continuous measuring of vertical profiles of temperature and water vapor density by means of a ground-based microwave radiometer[J]. Atmospheric Research, 2013,122:43-45.
[3] Dominique Ruffieux, Juerg Joss. Influence of radiation on the temperature sensor mounted on the swiss radiosonde[J]. J. Atmos. Oceanic Technology,2003, 20:1576-1582.
[4] Luers J. K.. Estimating the Temperature Error of the Radiosonde Rod Thermistor Under Different Environments[J]. J. Atmos. Oceanic Technology,1990,7:882-895.
[5] McMillin L., Uddstrom M., Coletti A.. A Procedure for Correcting Radiosonde Reports for Radiation Errors[J]. J. Atmos. Oceanic Technology,1992,9:801-811.
[6] James K. Luers, Robert E. Eskridge. Temperature Corrections for the VIZ and Vaisala

radiosondes[J]. Journal of Applied Meteorology,1995,34:1241-1253.
[7] Bomin Sun, Anthony Reale, Steven Schroeder, et al. Toward improved corrections for radiation-induced biases in radiosonde temperature observations[J]. Journal of geophysical research:Atmospheres,2013,18(10):4231-4243.
[8] Hoang M L,Verboven P,Baerdemaeker J De,et al.Analysis of the air flow in a cold store by means of computational fluid dynamics[J].International Journal of Refrigeration,2000,23:127-140.
[9] William L. Oberkampf, Timothy G. Trucano. Verification and validation in computational fluid dynamics[J]. Progress in aerospace science,2002,38:209-272.
[10] Francisco Domingo Molina-Aiz, Diego Luis Valera, Antonio Jesús Álvarez. Measurement and simulation of climate inside Almer´ıa-type greenhouses using computational fluid dynamics[J]. Agricultural and Forest Meteorology,2004, 125:33-51.
[11] NOAA. US Standard Atmosphere[M]. Washington DC:US Government Printing Office,1976:53-63.
[12] WMO. Guide to Meteorological Instruments and Methods of Observation (seventh edition)[M]. Geneva: Secretariat of WMO,2008:269-272.